

Basic Numerical Analysis on the GNVR Shape for an Airship

Kendrick Fernandes¹, Gaurak Phaldessai², Marvin Fernandes³

¹Department of Mechanical Engineering, Padre Conceicao College of Engineering, Goa, India.

²Professor, Department of Mechanical Engineering, Padre Conceicao College of Engineering, Goa, India.

³Professor, Department of Mechanical Engineering, Padre Conceicao College of Engineering, Goa, India.

Abstract - The Airship is among the first crafts to have attained a controlled flight and despite its age, is still relevant today. It is highly suitable for any application that needs a stable, relatively low cost, high endurance with low vibration and noise level. This paper illustrates the numerical analysis conducted on the shape used to construct an RC airship to simulate and study its behavior in the operating conditions. In essence, it also illustrates and validates the use of the GNVR shape which has been used in the Airship's construction.

Key Words: GNVR, Envelope, Lift, Pressure, Streamline, Vectors

1. INTRODUCTION

The Airship was the first craft to have attained a stable and controlled flight long before the Wright brothers in had flown their heavier-than-air Flyer 1. It is a "lighter than air" aircraft which uses the buoyancy force of its lifting gas as its main source of lift, due to the gas being less dense than air. The lifting gases primarily used are hydrogen and helium. This is in stark contrast to fixed wing aircrafts which generate their lift with the pressure difference arising from the air flowing across the wing. Even after more than a century, the basic airship design is highly suitable for any application that needs a stable, relatively low cost, high endurance platform with low vibration and noise level. The applications may include (but not limited too) surveillance of various atmospheric parameters for the scientific community, promotion activity for advertising firms, surface observation for extended time periods for coverage of sport events or precise dropping off payload for disaster relief operations.

1.1 Airships

Airships are generally classified into 3 types. These include as follows

1. Non-rigid: Large gas balloons with no internal structure to maintain the shape of its hull envelope. Its shape is maintained by internal overpressure.
2. Semi-rigid: Consists of a rigid lower keel construction and a pressurized envelope. The rigid keel could be attached directly to the

envelope or hung underneath it, aiding the envelope shape.

3. Rigid: a rigid structure-traditionally an aluminium alloy -holds up the form of the airship. This structure resembles a cage that encloses a series of balloons called gas cells, tailored to fit within the cylindrical space and secured in place by netting that transmits the lifting force of their gas to the structure.

1.2 Design of Airships

The most critical component of an airship is the Envelope. For the non-rigid design, it forms the structure, including the fabric that helps contain the lifting gas. It needs to allow gas expansion at higher altitudes as the air gets less dense the higher you climb. Further, the gas may also suddenly expand due to continuous irradiation from direct sunlight in a phenomenon called 'superheat'. This causes a sudden increase in buoyant force which can lead to loss of control.

The choice of envelope fabric is also the extremely crucial as it accounts to as much as 30-40% of the total gross weight of the airship (even for a non-rigid one). Some of the factors that need to be considered while selecting the material are high strength to weight ratio, resistance to environmental degradation, high tear resistance, Low permeability to reduce the leakage of gas, Low creep that ensures the envelope shape is maintained. Since the fabric needs to meet such a wide range of requirements, composite fabrics are favoured over an all-serving single purpose material. Composites fabrics mostly consist of a fabric substrate and coating film/s.

The shape of the envelope is crucial for the envelope. This dictates now the craft will behave once in flight and perform as per set design goals. Historically, Prolate spheroids are very similar to most airship designs and their mathematical shapes makes them excellent choices for studies as their flow-field is almost identical to that of a wing. Air flows over an airship body and accelerates to about the midpoint then decelerates over the aft portions until the flow meets at the trailing edge/ point to ensure there is no pressure discontinuity. The acceleration of the air particles causes the static pressure on the surfaces to drop below the static pressure in the free stream. Now, if the internal pressure is not enough, the nose of the

envelope will cave in due to the external pressure. Thus, the differential pressure about the centre line is about 10% more than the anticipated internal pressure. Other loads acting on the envelope are the circumferential (hoop) stresses and the longitudinal (buckling stress). Whenever there is an airflow around a body, a pressure distribution is set up over it. This gives rise to 'Lift-Drag' force pair. 'Lift' is perpendicular to the flow; which causes the body to move upwards. 'Drag' is parallel to the oncoming flow and is in the opposite direction of the relative motion of the body. Unlike other resistive forces, drag is wholly dependent on the fluid velocity and tries to decrease it with respect to the (relatively) solid object. Some of the various sub-components of this force are skin friction drag, form drag and lift-induced drag.

To take into account all these factors, the envelope shape must have a high volume to surface area ratio, high payload for maximum length and optimum slenderness ratio (overall length/ maximum diameter. From the work done by researchers, the GNVR shape is found to be optimum.^[5] This paper investigates the behaviour of the final airship shape in its design working condition using CFD simulations. This will validate if the assumptions arrived at during the design stage are held true.

2. Theoretical Calculations

From established procedure ^{[1][2]}, the basic design dimensions for the airship are tabulated in **Table 1**

Table 1: General sizing dimensions for the Airship

Length of the Airship (L)	3.099m
Maximum Diameter (D)	1.016m
Gas Volume (V)	3.2 m ³
Envelope length (L _e)	3.85 m
Envelope surface area (S _e)	12.37 m ²

With the general sizing completed, the stress analysis can be now carried out. The envelope must be able to withstand the following 3 stresses, (i) Stress due to internal pressure. (ΔP_{int}), (ii) Stress caused by differential pressure due to head. (ΔP_{head}) and (iii) Stress due to aerodynamic loading (ΔP_a). It must be noted that the internal pressure of the gas can never be exactly found as it varies within the entire volume. However, a good normalized estimate can be made by equating it to be 10% more than the maximum stagnation pressure (P_{max}). This pressure is defined at the stagnation point of the envelope-point at which velocity of streamline retards to zero. The various parameters were found using the equations given below.

$$\text{Maximum stagnation Pressure } (P_{max}) = \frac{1}{2} \times \rho_a \times v^2 \quad (\text{eq.1})^{[2]}$$

$$\text{Differential pressure at the centerline } (\Delta P_{int}) = (1 + 0.1) \times P_{max} \quad (\text{eq.2})^{[2]}$$

$$\text{Pressure due to aerodynamic loading } (\Delta P_a) = \frac{1}{2} \times \rho_a \times C_p \times v^2 \quad (\text{eq.3})^{[2]}$$

[Where C_p : - Pressure co-efficient varying from 0.3 to 0.35, here $C_p=0.33$]

$$\text{Hydrostatic pressure head } (\Delta P_{head}) = (\rho_a - \rho_{He}) \times g \times \frac{D}{2} \quad (\text{eq.4})^{[2]}$$

$$\text{Total Differential Pressure } (\Delta P) = \Delta P_{head} + \Delta P_a + \Delta P_{int} \quad (\text{eq.5})^{[2]}$$

$$\text{The Circumferential Unit Load (Hoop Load) } (L_{hoop}) = \Delta P \times \frac{D}{2} \quad (\text{eq. 6})^{[2]}$$

Evaluating longitudinal stresses ensures that the airship is safe from buckling along its longitudinal axis. This ensures that the envelope is always taut and has minimal wrinkles. To find this stress, the bending moment is required which is unique for each and every airship design. Since this is a much more complex field of analysis which is still being researched, it has been found by the following formula which has been mandated by the FAA (Federal Aviation Administration).

$$\text{Bending Moment (B.M)} = 0.029 \times \left[1 + \left(\frac{L}{D} - 4 \right) \times (0.5624L^{0.02} - 0.5) \right] \times (\rho_a uvVL^{0.25}) \quad (\text{eq.7})^{[2]}$$

Where,

u = gust velocity (25 ft/s as recommended by the FAA)

$$\text{Maximum Tensile Load } (L_t) = \frac{\Delta PR}{2} + \frac{BM}{\pi R^2} \quad (\text{eq.8})^{[2]}$$

Substituting Density of Air (ρ_a at 30°C) = 1.118 kg/m³, Density of Helium (ρ_{He} at 30°C) = 0.164kg/m³ and maximum design speed = 4m/s in above equations, the results are tabulated in **Table 2**.

Table 2: The values of the design parameters of the airship

Maximum stagnation Pressure (P_{max})	9 N/m ²
Differential pressure at the centerline (ΔP_{int})	10 N/m ²
Pressure due to aerodynamic loading (ΔP_a)	3 N/m ²
Hydrostatic pressure head (ΔP_{head})	5.624 N/m ²
Total Differential Pressure (ΔP)	18 N/m ²
Circumferential unit (hoop) load (L_{hoop})	13.6 N/ m
Bending Moment (B.M)	5.71 N-m
Maximum Tensile Load (L_t)	11.192 N/m

3. Numerical Analysis

To see how the airship would behave when subjected to working conditions and the behaviour of the air around it, a numerical analysis was conducted. This would ensure proper estimation for drag, surface forces and other various loading experienced by the airship. For this purpose, a 2-D numerical model was made with the help of 'ANSYS Fluent 14.5' to analyze the flow behaviour. For this, an external domain was created to capture the entire simulation. The dimensions of the envelope were chosen carefully to capture the results fully.

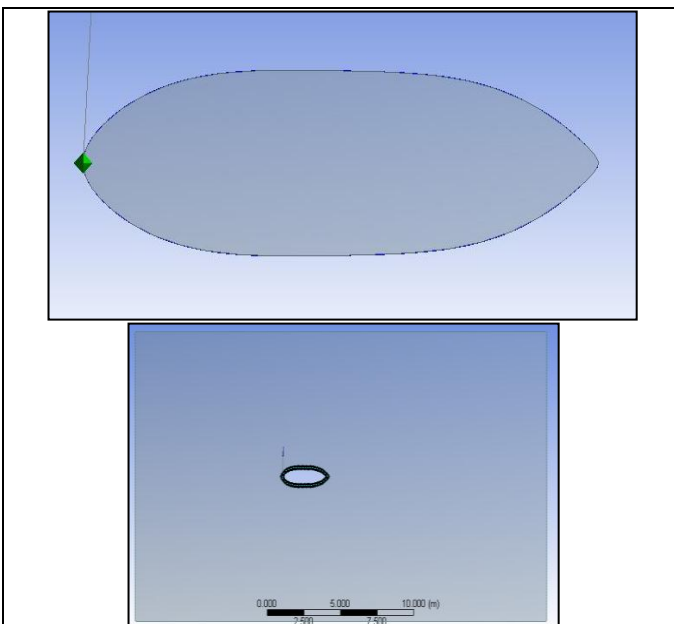


Figure 1: The simulation model and domain created in ANSYS along with its close-up

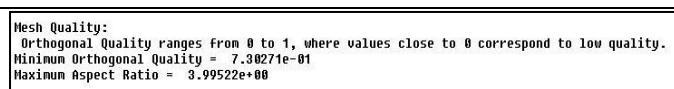


Figure 2: The mesh quality used for the model

Since the design deals with very low Mach speeds (As Mach 1 [347m/s] > 4m/s), the airflow can be considered to be incompressible. This assumption is valid up to speeds of Mach 0.3 (roughly 100m/s). Hence, a pressure-based solver is used since the convergence is faster and the simplifying assumptions don't affect the final answer by a substantial degree. The velocity formulation was kept absolute. As the model is set to face turbulence (as been asserted in literature) and the same has been noticed in the flow domain, K-epsilon flow model with standard wall conditions were set. The pressure and velocity coupling are done with the help of the 'SIMPLE' scheme option available in the said software. For the boundary conditions, one side of the domain was set as the inlet and the other was set as the outlet as shown in the **Figure 1**. The profile of the airship was set as wall boundary, velocity of air was set 4 m/s (as set in the design assumptions) and the outlet was

set as 'pressure outlet'. With all these parameters setup, the model was run and the result was found to converge on the 196th iteration.

Once the simulation converged to the answer, the results were recorded. The net force arises due to the interaction of the boundary layer of air and the airship wall. The point of interest is the viscous co-efficient of pressure. The drag force can be reasonably quantified with the help of the 'co-efficient of drag' of a given shape. Since the model is designed to fly at very low speeds, the drag can be approximated to be due to the viscous nature of the fluid. Hence, the drag co-efficient equals the viscous pressure co-efficient.

4. Results of the CFD Simulation

4.1 Variation of Static Pressure

Static pressure is simply defined as the weight of the fluid column acting on a given object, assuming the fluid is static. Due to the movement of air about shape, a pressure gradient is set up around it to minimize the loss of energy (conservation of energy). **Figure 3** shows the contour variation of static pressure over the profile along with a graph illustrating the same over its axial length. The pressure is seen to vary from -9.73 N/m² (dark blue) to 9.63N/m²(dark red). This corresponds accurately with theoretical values of stagnation pressure (refer **Table 2**)

The highest value of static pressure is at the nose tip. This stagnation point is highlighted as a red region in the contour plot, where the air velocity decelerates to zero; thus, implying complete momentum transfer. Moving along the profile, the pressure is observed to be negative and decreases to a global minimum (dark blue in contour plot). Then gradually, it starts increasing again towards the trailing edge to a local maximum. On attaining the local maximum, it dips slightly to a local minimum before it sharply increases to attain the atmospheric pressure towards the trailing edge. This behaviour is attributed the flow trying to maintain pressure continuity due to the Kutta Condition. In simple terms, the Kutta condition arises in cases of streamlined bodies with distinct leading and trailing edges.

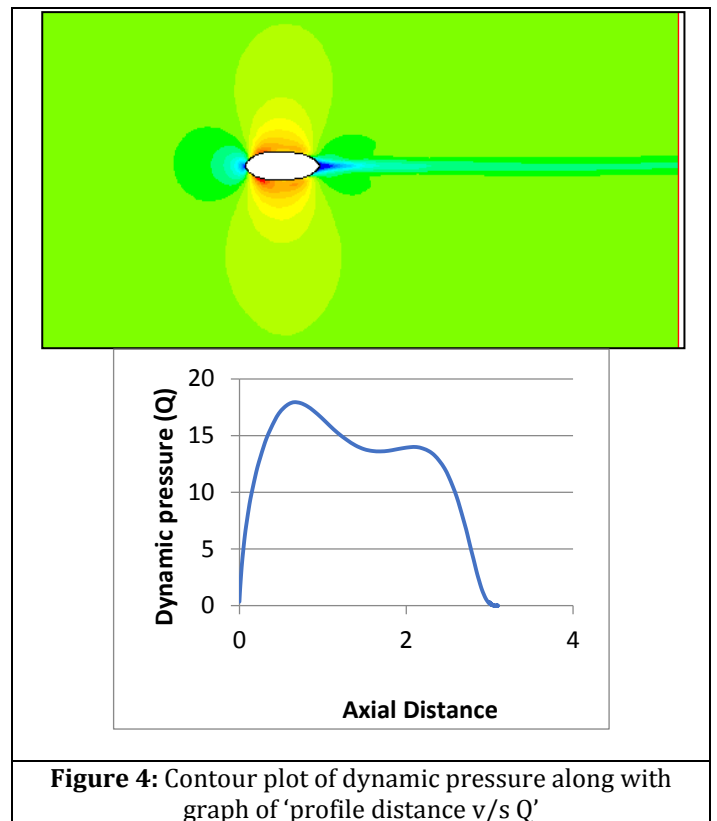
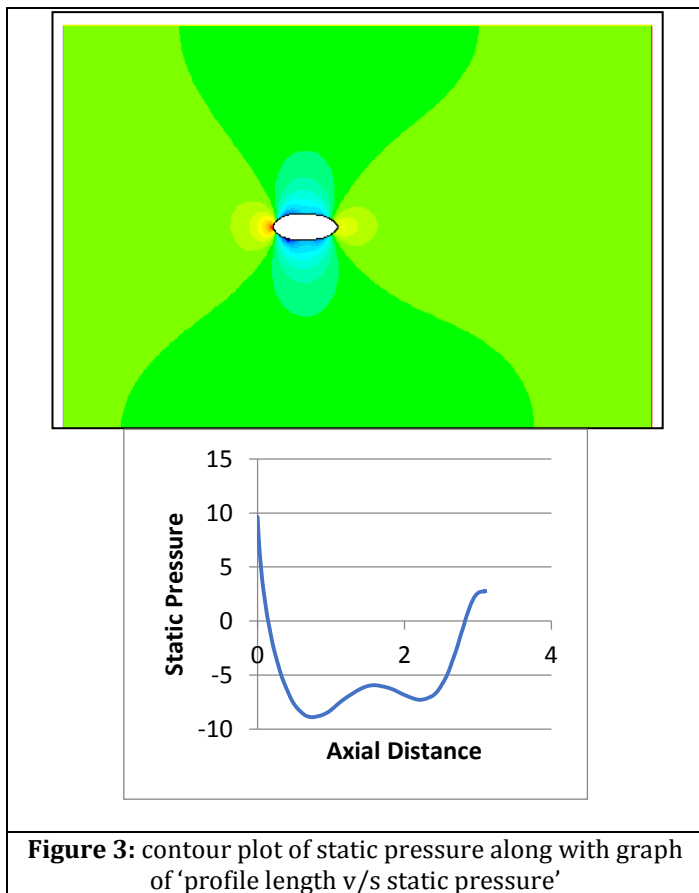


Figure 4: Contour plot of dynamic pressure along with graph of 'profile distance v/s Q'

Figure 3: contour plot of static pressure along with graph of 'profile length v/s static pressure'

This is hardly a surprise as all airship shapes use the 'NACA-66' airfoil design as a basis for their design and optimization. Another interesting consequence of the above condition is the slightly negative pressure gradient (shown in dark green) set up above and below the profile. This can be seen as a consequence of also maintaining Bernoulli's condition of streamline flow.

4.2 Variation in Dynamic Pressure

Dynamic pressure is associated with the pressure exerted by a moving fluid when it comes in contact with another object. It represents the kinetic energy associated with the fluid particles being transferred onto the said object. Figure 4 shows the variation of dynamic pressure (Q) over the shape along with the associated graph. It is noted that the pressure gradient is exactly the opposite compared to that of static pressure varying from $8.23 \times 10^{-5} \text{ N/m}^2$ (dark blue) to 17.87 N/m^2 (dark red).

The value of Q is minimum towards leading and trailing edges due to the separation of the airflow occurring ahead of the leading edge. Also, low Q values are observed in the wake left by the airship. This implies there is little to no back flow of air which would generate eddy's-and consequently, increase the drag force. The highest Q values are noticed just above and below the leading edge, due to the fact that the fluid velocity increases when passing over an air-foil shape, which increases it's kinetic energy.

4.3 Variation in Total pressure

Total pressure is the summation of the static and dynamic pressure, thus portraying the overall picture of the combined effect of these two quantities.

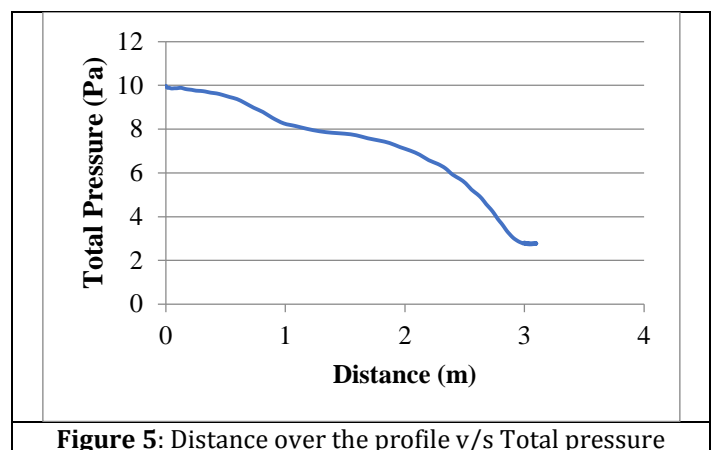


Figure 5: Distance over the profile v/s Total pressure

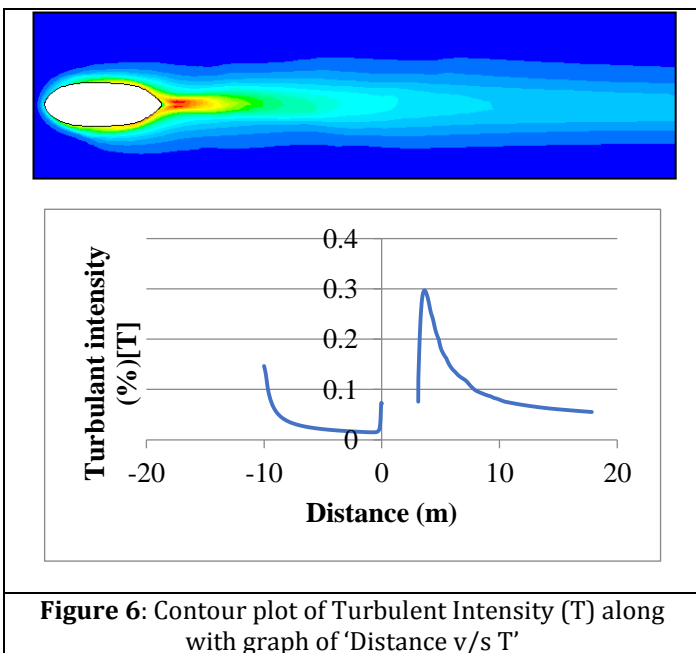
Figure 5 illustrates the plot of axial centreline distance of the profile v/s the total pressure. Studying the graph, a decreasing trend is observed from the leading edge till it evens out at a low value at the trailing edge. Thus, it can be safely stated that the static pressure always dominates over dynamic pressure in nearly all regions of the airship.

4.4 Variation in Turbulent Intensity

Turbulent intensity (T) gives a measure of how intense the wind velocity fluctuates. In this case, the fluctuations are due to the profile moving through the air, disturbing the streamlined flow it would otherwise possess. The contour plot in **Figure 6** showcases this behaviour while the associated graph gives a better visual understanding.

It is observed that closer to the leading edge, the intensity reduces to a minimum before spiking up to higher value at the nose. This behaviour is possibly due to the air slowing down and setting up the boundary layer about the profile. This value (around 0.075%, dark blue) is held throughout the profile and hits a maximum (around 0.3%, dark red) just after the trailing edge as seen as a red region in the contour. After this, it keeps on steadily decreasing in the wake region before levelling towards a local minimum at a sufficiently long distance.

Generally, values of 'T' less than 1% are usually desired while those above 5% are said to have high turbulent intensities [3][4], which increases drag. Considering the limited resources at hand, the fact that 'T' values mostly are between 0.05 and 0.3% are commendable.



4.5 Variation in Wall Shear Stress

Turbulent intensity has a very strong correlation with the wall shear stress(W) exerted on the profile. Wall shear stress occurs when the air layer closest to the profile adheres to the surface and thus, slows it down. This retardation occurs due to the friction present on the surface comes in contact with the fluid layer. In turn, a tangential force is exerted onto the profile walls. For any

aerodynamic shape, 'W' depends on the speed at which the body moves through it and the turbulence it experiences.

Studying **Figure 7**, moderately high stress values are noted about the boundary of the profile; mostly in the region after the leading edge and before the trailing edge. Since the values range between 0 N/m (dark blue) to 5.37×10^{-2} N/m (dark red), it does not contribute much to the overall stress as it is of the order of 1/100th of a decimal place. Thus, can safely be assumed to be accounted for in the initial design phase.

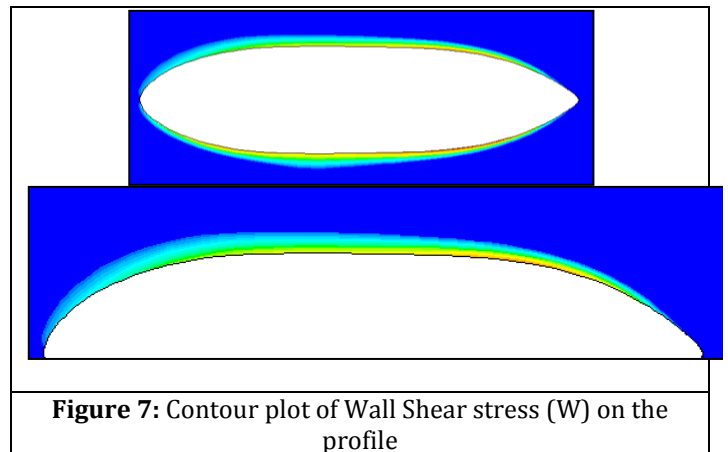


Figure 7: Contour plot of Wall Shear stress (W) on the profile

4.6 Variation in Velocity

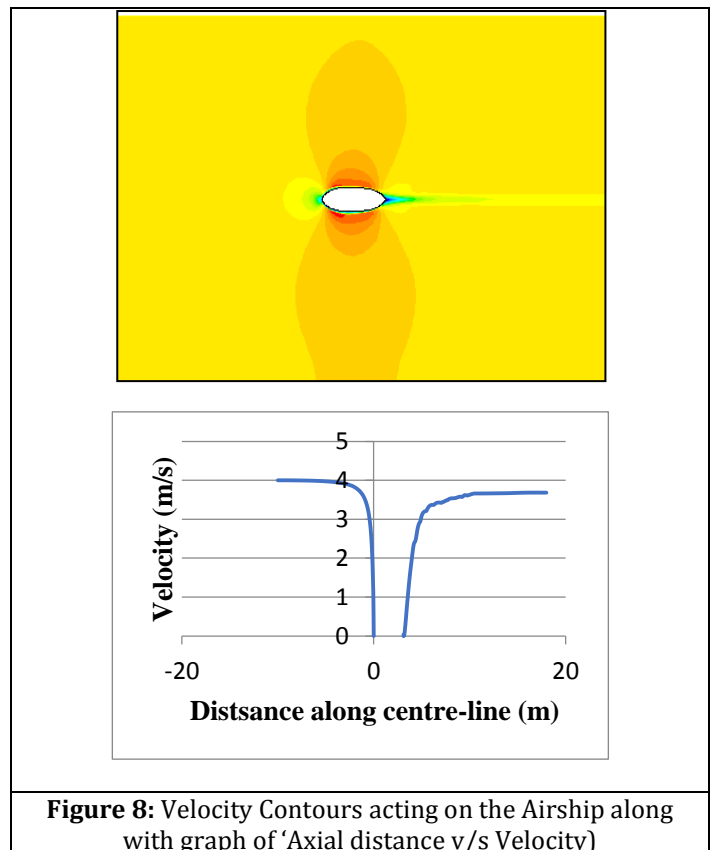


Figure 8: Velocity Contours acting on the Airship along with graph of 'Axial distance v/s Velocity'

With a design speed limit of 4m/s, the resulting velocity variation is observed along the axial centre-line and perpendicular to the centre-line; at the mid-point. **Figure 8** illustrates how the velocity varies over the entire region of simulation space while the graph shows the velocity variation in the axial direction. The overall velocity varies from 0m/s (dark blue) to 5.44m/s (dark red). In the Axial direction, the initial velocity is constant with a slight reduction observed at around 5 units from the leading edge. At around the 1unit mark, the speed starts to decrease asymptotically to zero; signifying the stagnation point has been attained. The gap of roughly 3 units is due to the presence of the profile. At around the 3.1unit mark-which is the trailing edge- the velocity is again seen to increase in a near asymptotic behaviour-though not as much as the aforementioned reduction-before stabilizing at around 3.5 to 3.6 m/s for the rest of the domain signifying the wake region left by the airship.

For the perpendicular velocity variation, the cross-section area at around 50% of the total length in the upward direction-as there is symmetry about the centreline- is considered (**Figure 9**). This data has been captured and plotted as a graph illustrated along with **Figure 9**. Initially, on moving from the surface of the profile upwards, no velocity is detected. This can be attributed to the near static, boundary layer set up around the profile. At around 0.505622 units from the surface, velocity is detected and is found to be slightly higher than the free stream velocity (around 4.87m/s). This value increases to a maximum 5m/s at around a height of 0.73 following which, it gradually decreases at higher vertical distances until it steadies to the free stream velocity at around a height of 8 units. The velocity increase can be attributed to Bernoulli's equation condition being satisfied.

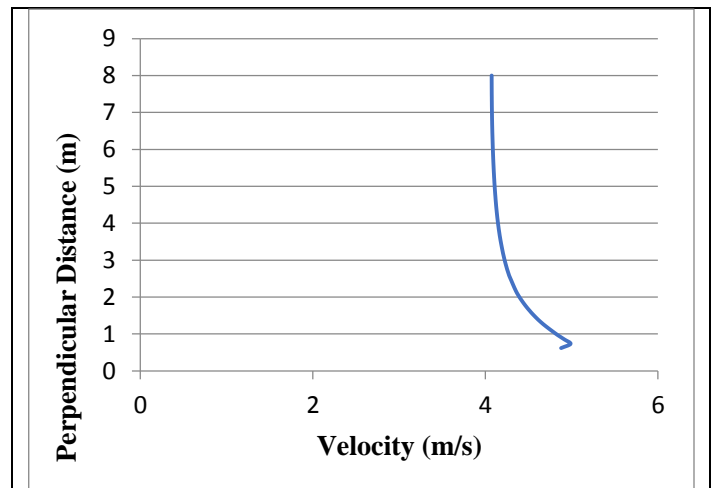
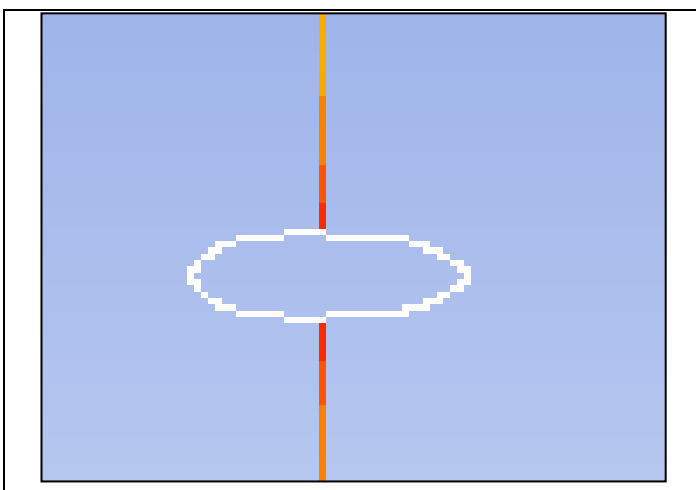


Figure 9: The location at which the perpendicular velocity gradient was studied along with graph of 'Velocity v/s perpendicular distance'

4.7 Velocity Streamlines

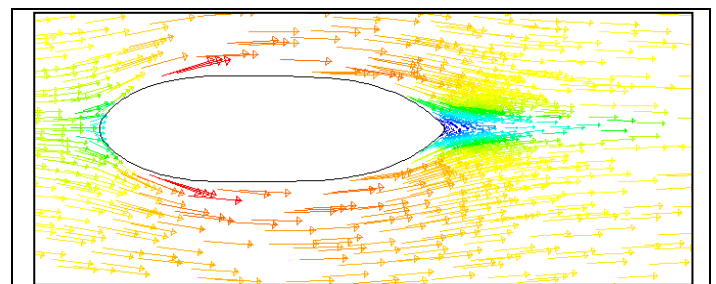


Figure 10: Vector plot of airflow

Now the behaviour of the streamlines has to be investigated. This is exceedingly important as it illustrates how aerodynamic the chosen shape is and how the air interacts with it. **Figure 10** displays the variation of the velocity vectors between 2.12×10^{-3} m/s to 5.44m/s around the shape. Note the 2 regions of high vector density, which corresponds with the stagnation point (leading edge) and the region of flow convergence (after the trailing edge). The region of flow convergence is of more importance for this project as any back-flow would result in an unwanted increase in drag. This would imply that the design is yet to be optimized.

Observing the leading edge in **Figure 11**, a region of disturbance is created as the vectors approach the profile. This is due to the flow being divided into 2 parts while still trying to maintain their streamline flow. Hence, oncoming vectors tend to direct themselves either above or below the oncoming surface to maintain slow continuity. The vectors in the mentioned region are seen to slow down drastically to a halt at the nose, thus exerting maximum pressure there. The vectors that move along the contours are briefly

seen to speed up due to Bernoulli's condition. As stated earlier, the static pressure was found to be quite low in the areas just above and below the leading edge. As a consequence, the velocity of air must increase to offset this deficiency. As the vectors converge as seen in the trailing edge of **Figure 11**, they attain the free stream velocity; except those in line of the flying path of the airship which caused the wake.

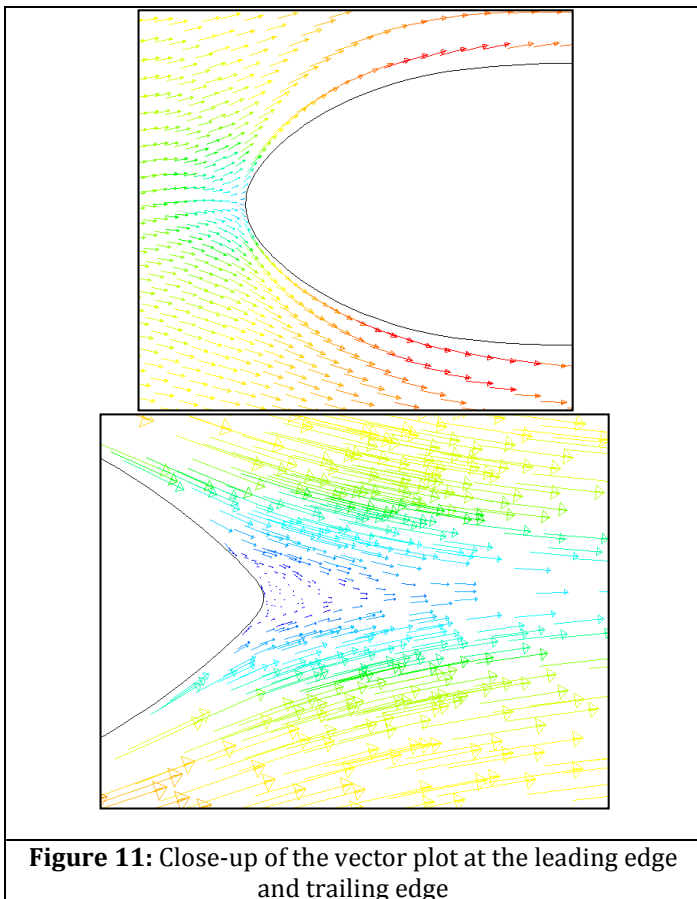


Figure 11: Close-up of the vector plot at the leading edge and trailing edge

The vector values in the wake (shown in blue) are much lower compared to the stream velocity, which may be due to the turbulence. They continue to decrease on moving closer to the trailing edge. Also, all of them seem to be moving away from the trailing point indicating streamline flow. However, the possibility of back-flow eddies cannot be neglected just under the simplistic assumptions that the vectors are not observed. Further magnification is needed to check the direction of flow just after the said region, which is provided in **Figure 12**. Observe that the vectors are now reduced to a point indicating little to no flow of air in this area. Ordinarily, we can say the velocity of flow here is zero. This is a very promising result as the absence of the 'eddy backflow' implies the drag faced by the airship is not due to any 'bad airflow' behaviour in the wake region.

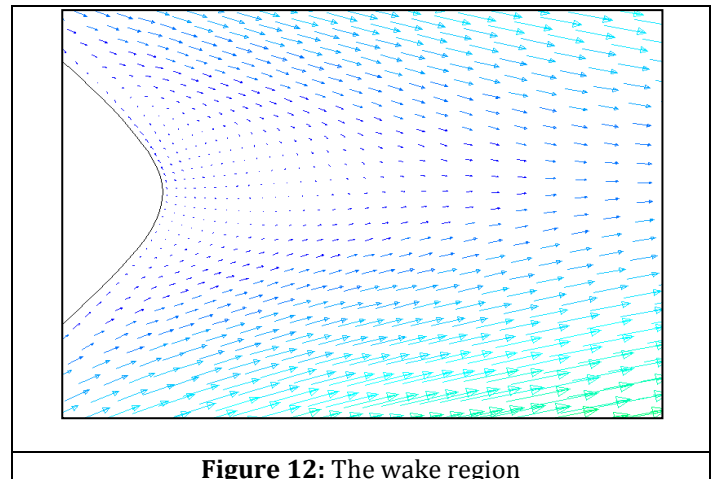


Figure 12: The wake region

5. Conclusion

The profile shape of the airship has been modelled on 'ANSYS Fluent 14.5' and simulated under its design conditions. The various stress parameters obtained from the simulation closely match those from the theoretical design phase. Initial analysis on turbulence has also found it to be within limits as stipulated by literature. While the turbulence does cause wall shear stress, its magnitude is so small that it is said to be considered in the initial design phase itself. Examination of the vector air flow has shown that no eddy currents are formed. Thus, it can be concluded that the design of the given airship-within the given constraints-is structurally and aerodynamically sound. Hence, the GNVR shape has been validated.

References

- [1] Amol Gawale, Amool Raina, Rajkumar Pant, Yogendra Jahagirdar. 'Design, Fabrication and Operation of Remotely Controlled Airships in India.', Indian Institute of Technology Bombay; Research Institute for Model Aeronautics.
- [2] Amol Gawale and Rajkumar S. Pant, IITB. 'Design, fabrication and flight testing of remotely controlled airship.'
- [3] GE Carichner, LM Nicolai 'Fundamentals of Aircraft and Airship Design: volume II, Airship Design', American Institute of Aeronautics and Astronautics, 2013
- [4] G.A. Khoury and J.D. Gillet, Cambridge Aerospace series, (1999). 'Airship technology'